Proceedings of ISINN-30, JINR, E3-2024-42, Dubna, 2024, p.128 – 135

Prompt Fission Neutron Spectra of ^{240}Pu(n,F)

V.M. Maslov*

220025 Minsk, Byelorussia

*E–mail: mvm2386@yandex.ru

Variation of fission neutron spectra of ^{240}Pu(*sf*) and ^{240}Pu(*n,F*) for $E_n \lesssim 20$ MeV is predicted. Features of angle-integrated prompt fission neutron spectra (PFNS) of ^{240}Pu(*n,F*) stem from simultaneous analysis of data for ^{238}U(*n,F*), ^{239}Pu(*n,F*) and available data on ^{240}Pu(*n,F*) PFNS. The data on average energies $\langle E \rangle$ of ^{240}Pu(*n,F*) PFNS support the approach pursued in case of ^{238}U(*n,F*) and ^{239}Pu(*n,F*). Soft influence of exclusive neutron spectra on PFNS is observed in case of ^{240}Pu(*n,F*) and ^{240}Pu(*n,nf*)^1 at E_n~7÷8 MeV. The largest relative amplitude of exclusive neutron spectra ^{240}Pu(*n,xnf*)^1 is envisaged at E_n~6÷6.25 MeV. PFNS of ^{240}Pu(*n,F*) are harder than those of ^{238}U(*n,F*), but softer than PFNS for ^{239}Pu(*n,F*). The ^{240}Pu(*n,F*) PFNS shape is rather close to that of ^{239}Pu(*n,F*), though the contribution of pre-fission neutrons is relatively higher. Exclusive neutron spectra (*n,xnf*)$^{1,..x}$ are consistent with σ(*n,F*) of $^{237-240}$Pu(*n,F*), as well as neutron emissive spectra of ^{239}Pu(*n,xn*) at E_n~14 MeV. We predict the ^{240}Pu(*n,xnf*)$^{1,..x}$ exclusive pre-fission neutron spectra, exclusive neutron spectra of ^{240}Pu(*n,xn*)$^{1,..x}$ reactions, average total kinetic energy TKE of fission fragments and products, partials of average prompt fission neutron number and observed PFNS of ^{240}Pu(*n,F*).

PACS: 24.75.+i; 25.40.-h; 25.85.Ec

INTRODUCTION

Since the recent paper [1] on ^{238}U(*n,F*), ^{239}Pu(*n,F*) and ^{240}Pu(*n,F*) PFNS, became available fragmentary data on PFNS and its $\langle E \rangle$ for $0.8 \lesssim \varepsilon \lesssim 10$ MeV prompt fission neutron energy interval [2]. The PFNS shapes of ^{238}U(*n,F*) [1, 3] and ^{239}Pu(*n,F*) [1, 4, 5] reactions are very much different from each other, the PFNS of ^{240}Pu(*n,F*) lying in-between. It seems the contribution of pre-fission neutrons for ^{240}Pu(*n,F*) is lower than in case of ^{238}U(*n,F*), but higher than in case of ^{239}Pu(*n,F*) and vice versa as regards the prompt fission neutrons emitted from fragments. At $E_n \gtrsim E_{nnf}$, E_{nnf} being (*n,nf*) reaction threshold, pre–fission neutrons influence the partitioning of fission energy between excitation energy and TKE of fission fragments. Analysis of measured data for ^{238}U(*n,F*) and ^{240}Pu(*n,F*) allows to demonstrate sensitivities of PFNS shape near (*n,xnf*) reaction thresholds to the exclusive pre-fission neutron spectra. Those for ^{238}U(*n,F*) PFNS [3] are strongly supported by the measured data [6] with minor exceptions at E_n~ 8÷12 MeV. In that case strong influence of ^{238}U(*n,nf*)^1 excusive neutron spectra on PFNS at E_n~ 7 MeV and E_n~ 7÷8 MeV is demonstrated [1], while it might be predicted for the ^{240}Pu(*n,F*) and ^{240}Pu(*n,nf*)^1. PFNS for ^{239}Pu(*n,F*) [1, 4, 5] are strongly supported by measured data [7, 8]. Much softer influence of ^{240}Pu(*n,nf*)^1 excusive neutron spectra on PFNS at $E_n \gtrsim E_{nnf}$ is due to exceptionally high contribution of first chance ^{240}Pu(*n,f*) fission reaction σ(*n,f*) to observed σ(*n,F*).

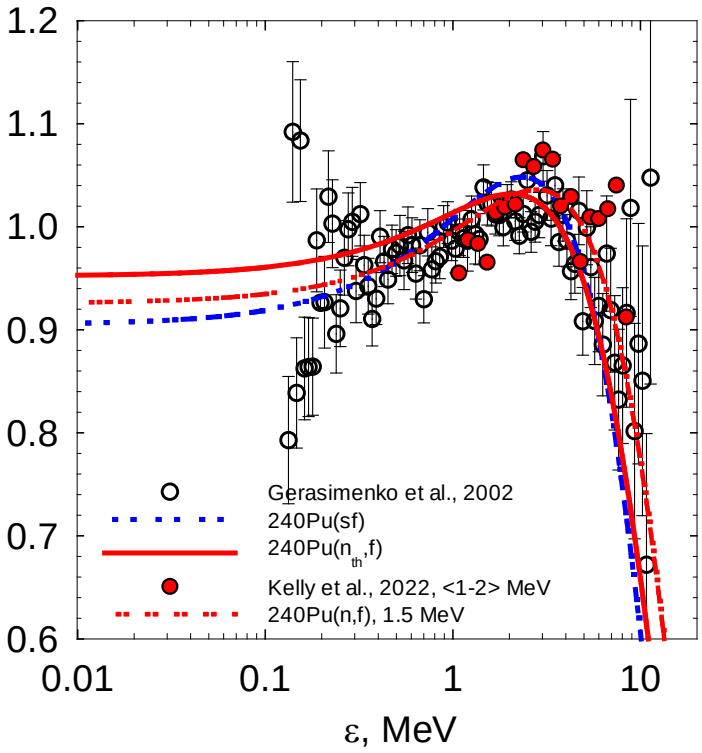

Fig.1. PFNS of ^{240}Pu(n_{th},f) and ^{240}Pu(n_{th},f) relative to Maxwellian with $\langle E \rangle$=2.0564 MeV.

^{240}Pu(n,f) PROMPT FISSION NEUTRON SPECTRA

The reliability of the modelling of PFNS for neutron-induced fission of ^{239}Pu might be augmented by analysis of ^{239}Pu(n_{th},f)&^{240}Pu(sf) data sets. Similar augmentation is possible for a pair of fission reactions ^{241}Pu(n_{th},f)&^{242}Pu(sf). In reaction ^{239}Pu(n_{th},f) neutron yield comes mostly from $J^{\pi} = 0^{+}$ states, same as in ^{240}Pu(sf) spontaneous fission neutron spectra (SFNS). Comparison of PFNS of ^{239}Pu(n_{th},f) and SFNS of ^{240}Pu(sf) [9] in [1] shows that at ε<0.2 MeV PFNS and SFNS of fissioning nuclide ^{240}Pu depend only weakly on the excitation energy, while at $\varepsilon \gtrsim \langle E \rangle$ the PFNS of ^{239}Pu(n_{th},f) is much harder than SFNS. The same happens in case of calculated ^{241}Pu(n_{th},f) PFNS and ^{242}Pu(sf) [9]. For a pair ^{240}Pu(n_{th},f)&^{241}Pu(sf) such augmentation is hardly possible, though some guidance stems from pair of spectra of ^{240}Pu(n_{th},f) &^{240}Pu(sf).

Major parameters of ^{240}Pu(n_{th},f) PFNS modelling α, α_1 and E_F^{pre} define the kinetic energy of the fragments at the moment of prompt fission neutron emission [1, 3–5]. Lowering of PFNS $\langle E \rangle$ for ^{240}Pu(n_{th},f) relative to $\langle E \rangle$ of ^{239}Pu(n_{th},f) is due to binding energies B_n and TKE values differences[1, 4, 5]. Figure 1 shows ^{240}Pu(n_{th},f) PFNS and SFNS of ^{240}Pu(sf) [9], the former being harder at $\varepsilon \gtrsim \langle E \rangle$. The ^{239}Pu($n$,$f$) PFNS data at E_n~ 1.5 MeV [2] are consistent with hardening of the calculated PFNS with increase of E_n.

(*n,xnf*) PROMPT FISSION NEUTRON SPECTRA

At $E_n > E_{nnf}$ integral prompt fission neutron spectra $S(\varepsilon, E_n)$ is a superposition of exclusive spectra of pre-fission neutrons, $(n,nf)^1$, $(n,2nf)^{1,2}$, $(n,3nf)^{1,2,3}$ – $d\sigma^k_{nxnf}(\varepsilon, E_n)/d\varepsilon$ (x= 0,1,2, 3; k=*1,…,x*), and spectra of prompt fission neutrons, emitted by fission fragments, $S_{A+1-x}(\varepsilon,E_n)$:

$$
\begin{aligned}
&S(\varepsilon,E_n) = \widetilde{S}_{A+1}(\varepsilon,E_n) + \widetilde{S}_{A}(\varepsilon,E_n) + \widetilde{S}_{A-1}(\varepsilon,E_n) + \widetilde{S}_{A-2}(\varepsilon,E_n) = \\
&\nu_p^{-1}(E_n)\cdot\{\ \nu_{p1}(E_n)\cdot\beta_1(E_n)S_{A+1}(\varepsilon,E_n) + \nu_{p2}(E_n - \langle E_{nnf}\rangle)\beta_2(E_n)S_A(\varepsilon,E_n) + \\
&+\beta_2(E_n)\frac{d\sigma^1_{nnf}(\varepsilon,E_n)}{d\varepsilon} + \nu_{p3}(E_n - B_n^A - \langle E^1_{n2nf}\rangle - \langle E^2_{n2nf}\rangle)\beta_3(E_n)S_{A-1}(\varepsilon,E_n) + \beta_3(E_n)\cdot \\
&\left[\frac{d\sigma^1_{n2nf}(\varepsilon,E_n)}{d\varepsilon} + \frac{d\sigma^2_{n2nf}(\varepsilon,E_n)}{d\varepsilon}\right] + \nu_{p4}(E_n - B_n^A - B_n^{A-1} - \langle E^1_{n3nf}\rangle - \langle E^2_{n3nf}\rangle - \langle E^3_{n3nf}\rangle)\cdot \\
&\beta_4(E_n)S_{A-2}(\varepsilon,E_n) + \beta_4(E_n)\left[\frac{d\sigma^1_{n3nf}(\varepsilon,E_n)}{d\varepsilon} + \frac{d\sigma^2_{n3nf}(\varepsilon,E_n)}{d\varepsilon} + \frac{d\sigma^3_{n2nf}(\varepsilon,E_n)}{d\varepsilon}\right]\ \}.
\end{aligned}
\tag{1}
$$

In Eq. 1 $\widetilde{S}_{A+1-x}(\varepsilon,E_n)$ is contribution of x-chance fission to the observed PFNS, $\langle E^k_{nxnf}\rangle$ – average energy of k-th neutron of (*n,xnf*) reaction with spectrum $d\sigma^k_{nxn}(\varepsilon,E_n)/d\varepsilon$, $k \le x$, spectra $S(\varepsilon,E_n)$, $S_{A+1-x}(\varepsilon,E_n)$ and $d\sigma^k_{nxn}(\varepsilon,E_n)/d\varepsilon$ are normalized to unity, $\beta_x(E_n) = \sigma_{n,xnf}(E_n)/\sigma_{n,F}(E_n)$ – contribution of x-th fission chance to the observed fission cross section, $\nu_p(E_n)$ observed average number of prompt fission neutrons, $\nu_{px}(E_{nx})$ – average number of prompt fission neutrons, emitted by $^{241\text{-}x}$Pu nuclides. Spectra of prompt fission neutrons, emitted from fragments, $S_{A+1-x}(\varepsilon,E_n)$, as proposed in [10], were approximated by the sum of two Watt [11] distributions with different temperatures, the temperature of light fragment being higher. Exclusive neutron spectra $(n,xnf)^{1,..x}$ are calculated simultaneously with σ(*n,F*) of $^{237-240}$Pu(*n,F*), as well as neutron emissive spectra of ^{239}Pu(*n,xn*) at ~14 MeV [4, 5].

Analysis of prompt fission neutron spectra of ^{238}U(*n,F*) [1, 3, 12, 13] and ^{239}Pu(*n,F*) [1, 4, 5] confirmed strict correlations of a number observed data structures with $(n,xnf)^{1...x}$ pre- fission neutrons. Pre-fission neutron spectra turned out to be quite soft as compared with neutrons emitted by excited fission fragments. The net outcome of that is the decrease of $\langle E\rangle$ in the vicinity of the (*n,xnf*) thresholds. The amplitude of the $\langle E\rangle$ variation is much higher in case of ^{238}U(*n,F*) as compared with ^{239}Pu(*n,F*) [1]. This peculiarity is due to differing emissive fission contributions in ^{239}Pu(*n,F*) and ^{238}U(*n,F*). The increase of the average energies of the exclusive pre-fission neutron spectra is faster in case of ^{239}U(*n,F*) than in case of ^{239}Pu(*n,F*), in consistency with measured data. The differential PFNS are susceptible to systematic errors of different origin. In ratios of PFNS, especially of draft PFNS data, these errors may be cancelled

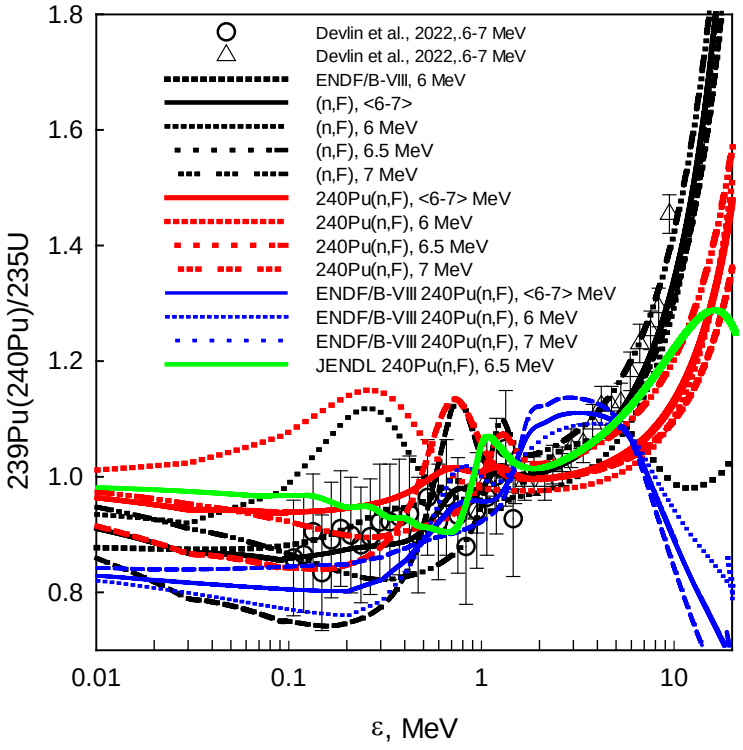

Fig.2. Ratios of PFNS ^{240}Pu(n,F)/^{235}U(n,F) and ^{239}Pu(n,F)/^{235}U(n,F) at E_n~6÷7 MeV.

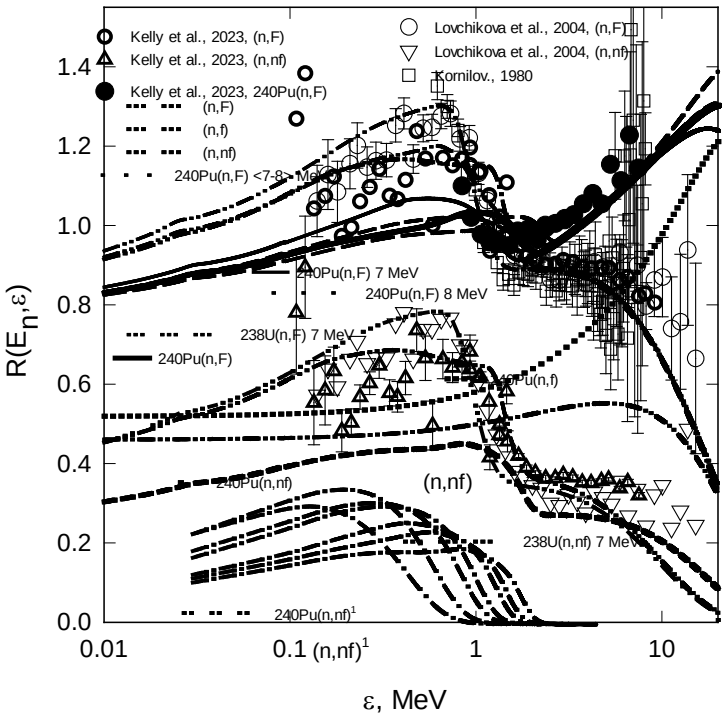

Fig.3. PFNS of ^{240}Pu(n,F) and ^{238}U(n,F) relative to Maxwellian with $\langle E \rangle$=2.0242 MeV, E_n~7÷8 MeV.

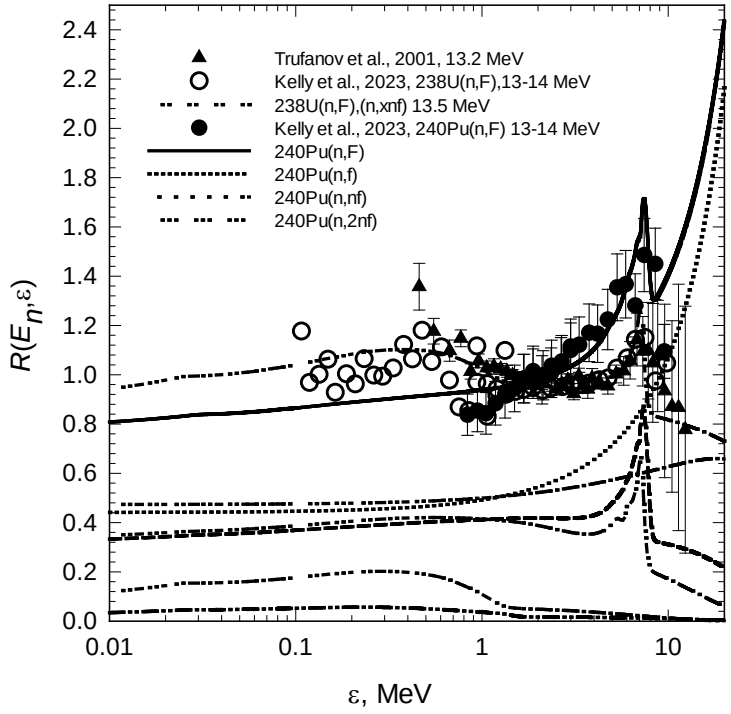

Fig.4. PFNS ^{240}Pu(*n,F*) and ^{238}U(*n,F*) distributions relative to Maxwellian with $\langle E \rangle$=2.0415 MeV, E_n~13÷14 MeV.

[6, 14]. Figure 2 shows the ^{239}Pu(*n,F*)/^{235}U(*n,F*) and ^{240}Pu(*n,F*)/^{235}U(*n,F*) ratios of PFNS for rather wide range of E_n~ 6÷7 MeV. In case of ^{239}Pu(*n,F*)/^{235}U(*n,F*) ratio the data of [4, 5], when averaged over E_n~ 6÷7 MeV range are compatible with measured data [6, 14]. The averaged ^{240}Pu(*n,F*)/^{235}U(*n,F*) ratio is very much different from that of ^{239}Pu(*n,F*)/^{235}U(*n,F*). The ^{239}Pu(*n,F*)/^{235}U(*n,F*) ratios of differential PFNS at E_n~ 6, 6.5 and 7 MeV fluctuate around averaged values. The ^{240}Pu(*n,F*)/^{235}U(*n,F*) ratios at E_n~ 6, 6.5 and 7 MeV are also very much different from those of ^{239}Pu(*n,F*)/^{235}U(*n,F*). That difference is due to shape of exclusive pre-fission (*n,nf*) neutron spectra and $\beta_x(E_n) = \sigma_{n,xnf}(E_n)/\sigma_{n,F}(E_n)$ values. The ^{240}Pu(*n,F*)/^{235}U(*n,F*) averaged ratios and ratios at E_n~6, 6.5 and 7 MeV of ENDF/B-VIII.0 [15] and JENDL-4.0 [16] are much discrepant with our estimates. That might be due at least to the same reasons as in case of our calculated ^{239}Pu(*n,F*)/^{235}U(*n,F*) and ^{240}Pu(*n,F*)/^{235}U(*n,F*). In the next energy range of E_n~ 7÷8 [6] the fluctuations of differential PFNS at E_n~ 7, 7.5 and 8 MeV are damped both in case of ^{239}Pu(*n,F*)/^{235}U(*n,F*) and ^{240}Pu(*n,F*)/^{235}U(*n,F*) ratios. The ^{240}Pu(*n,F*) PFNS is compared with ^{238}U(*n,F*) PFNS measured [6, 17, 18] and calculated [1, 13] data on Fig. 3. Obviously, the shapes of ^{240}Pu $(n,nf)^1$ exclusive pre-fission neutron spectra are much different from those of ^{238}U$(n,nf)^1$. The PFNS of ^{240}Pu(*n,F*) at E_n~ 7, 7.5 and 8 MeV are not very much dependent upon excitation energy, since the threshold of ^{240}Pu(*n,2n*) is lower than that of ^{238}U(*n,2n*). That influences competition of $(n,nf)^1$ and $(n,2n)^{1,2}$ reactions. At $E_n \gtrsim E_{n2nf}$ integral emission spectrum of $(n,nX)^1$ reaction, $d^2\sigma^1_{nnx}(\varepsilon, E_n)/d\varepsilon$, could be represented as a sum of compound and weakly dependent on neutron emission angle pre-equilibrium components, and phenomenological function, modelling energy and angle dependence of neutron spectra, relevant for the ^{240}Pu excitations of 1~6 MeV.

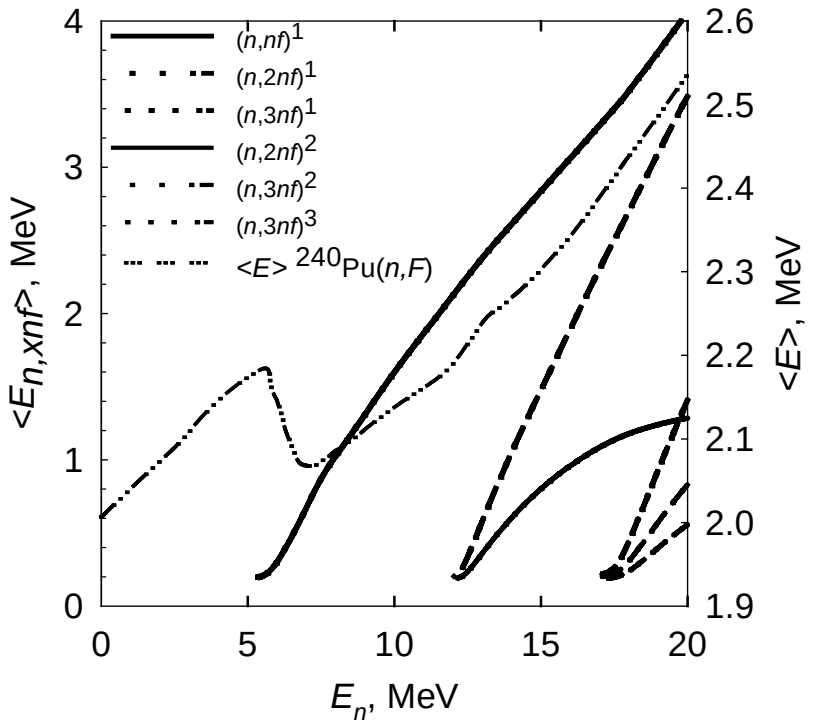

Fig.5. Average energy $\left\langle E^{k}_{nxnf} \right\rangle$ of ^{240}Pu(n,F) PFNS.

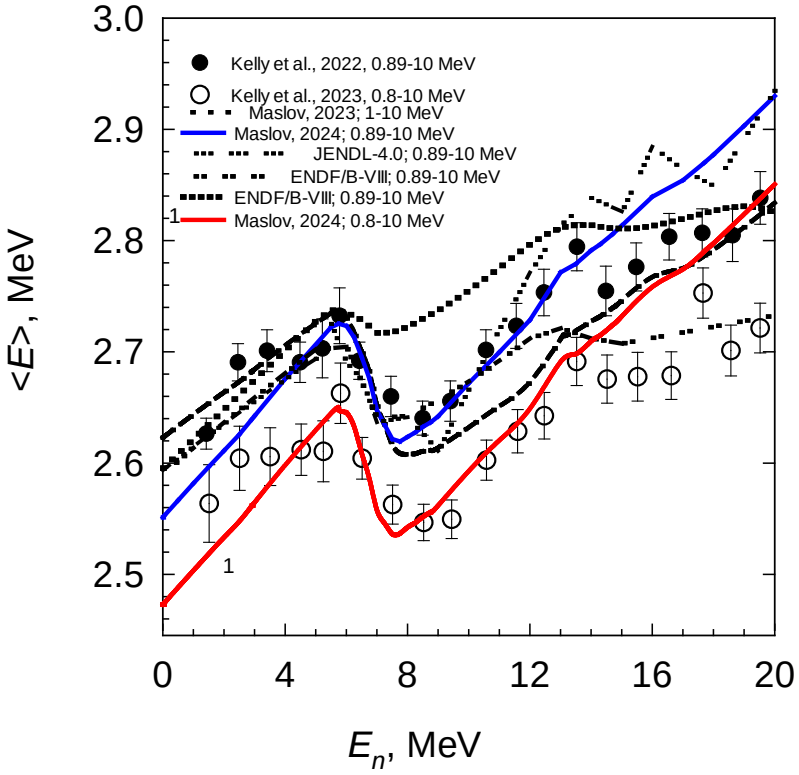

Fig.6. Average energy $\left\langle E \right\rangle$ of ^{240}Pu(n,F) PFNS.

Angle-averaged $\langle\omega(\theta)\rangle_\theta$ function, $\omega(\theta)$ [5], is approximated as $\langle\omega(\theta)\rangle_\theta \approx \omega(90^o)$, then integral spectrum equals

$$\frac{d\sigma^1_{nnx}(\varepsilon,E_n)}{d\varepsilon} \approx \frac{d\widetilde{\sigma}^1_{nnx}(\varepsilon,E_n)}{d\varepsilon} + \sqrt{\frac{\varepsilon}{E_n}}\frac{\langle\omega(\theta)\rangle_\theta}{E_n-\varepsilon} \quad (2)$$

Figure 4 compares calculated and measured PFNS of ^{238}U(*n,F*) [6, 19] and ^{240}Pu(*n,F*) [2] at E_n~ 13÷14 MeV. The $\widetilde{S}_{241-x}(\varepsilon,E_n)$ components of PFNS, shown on Fig. 4 reveal high contribution of $\widetilde{S}_{241}(\varepsilon,E_n)$ at $\varepsilon \gtrsim \langle E\rangle$. The contribution of $\widetilde{S}_{240}(\varepsilon,E_n)$ is lower than respective second-chance contribution of $\widetilde{S}_{238}(\varepsilon,E_n)$. The contributions of $d\sigma^1_{n2nf}(\varepsilon,E_n)/d\varepsilon$ and $d\sigma^2_{n2nf}(\varepsilon,E_n)/d\varepsilon$ to the third-chance fission component $\widetilde{S}_{239}(\varepsilon,E_n)$ are much lower than in case of ^{238}U(*n*,2*nf*) reaction, as predicted in [3].

Pre-fission neutrons define PFNS shape of ^{240}Pu(*n,F*) at E_n~ E_{nnf} –20 MeV. The variations of observed mean energies $\langle E\rangle$ for $0 \lesssim \varepsilon \lesssim 30$ MeV in the vicinity of (*n,xnf*) reaction thresholds, are shown on Fig. 5. The excitation energy residual nuclides, after emission of (*n,xnf*) neutrons, is decreased by the binding energy of emitted neutron B_{nx} and its average kinetic energy:

$$U_x = E_n + B_n - \sum_{x,1\le k\le x}(< E^k_{nxnf}(\theta) > + B_{nx}). \quad (3)$$

Values $\langle E^k_{nxnf}\rangle$ of exclusive spectra of $(n,xnf)^{1,..x}$ pre-fission neutrons are shown on Fig. 5.

The amplitude of variations of $\langle E\rangle$ for ^{240}Pu(*n,F*) PFNS for $0.8 \lesssim \varepsilon \lesssim 10$ MeV is supported by measured data of [2], preliminary $\langle E\rangle$ for $0.89 \lesssim \varepsilon \lesssim 10$ MeV range are also compatible with present PFNS (see Fig. 6). The estimate [1] of $\langle E\rangle$ for $1 \lesssim \varepsilon \lesssim 10$ MeV exhibits lowering, starting from $E_n \gtrsim 8$ MeV, by ~100 keV. The variations of average PFNS energy due to exclusive spectra of $(n,xnf)^{1,..x}$ neutrons are the same as predicted in [1], the systematic lowering is due to erroneous $S_{239}(\varepsilon,E_n)$ of ^{238}U(*n,f*) reaction. The net effect of these procedures is the adequate approximation of angular distributions of ^{238}U $(n,nX)^1$ first neutron inelastic scattering in continuum which corresponds to U=1~6 MeV excitations for E_n up to ~20 MeV.

CONCLUSION

Predicted distribution of fission energy of ^{240}Pu(*n,F*) reaction between fission fragments kinetic energy, their excitation energy and pre-fission neutrons is compatible with available data on TKE shape of fission fragments and products [1], prompt neutron number, observed PFNS and their average energies.

The estimates of $\langle E\rangle$ for ^{240}Pu(*n,F*) are strongly correlated with PFNS shape, which is not the case in [15, 16]. The influence of exclusive neutron spectra of ^{240}Pu$(n,nf)^1$ and ^{240}Pu$(n,2nf)^{1,2}$ which they exert on $\langle E\rangle$ in case of ^{240}Pu(*n,F*) is much stronger than in case of

^{239}Pu(*n*,*F*), but weaker than in case of ^{238}U(*n*,*F*) PFNS. The correlations of $\langle E \rangle$ variations for ^{240}Pu(*n*,*F*) in the vicinity of ^{240}Pu(*n*,*nf*) and ^{240}Pu(*n*,*2nf*) thresholds, with PFNS shape and values of $\beta_x(E_n) = \sigma_{n,xnf} / \sigma_{n,F}$, exclusive neutron spectra $(n,xnf)^{1...x}$ and calculated and observed TKE are established. The abrupt lowering of measured $\langle E \rangle$ of ^{240}Pu(*n*,*F*) PFNS at $E_n \gtrsim E_{n2nf}$ is incompatible with rather mild contribution of ^{240}Pu(*n*,2*nf*) to calculated PFNS.

REFERENCES

1. Maslov V.M. Physics of Particles and Nuclei Letters, 20 (4), 565 (2023).
2. Kelly K. J., Devlin M., O'Donnell J. M. et al. LANSCE CoGNAC and Chi-Nu Experimental Updates—Nuclear Data Week(s) 2023 (CSEWG-USNDP-NDAG), November, 2023; https://indico.bnl.gov/event/18701/contributions/82692/ . LA-UR-23-33042.
3. Maslov V.M., Porodzinskij Yu. V., Baba M., Hasegawa A., Kornilov N.V., Kagalenko A.B. and Tetereva N.A. Phys. Rev. C, 69, 034607 (2004).
4. Maslov V.M. Physics of Atomic Nuclei, 86 (5), 627 (2023).
5. Maslov V.M. Physics of Particles and Nuclei Letters, 20 (6), 1373 (2023).
6. Kelly K. J., Devlin M. J., O'Donnell M. et al. Phys. Rev. C, 108, p. 024603(1) – 024603 (15) (2023).
7. Kelly K. J., Devlin M., O'Donnel J.M. et al. Phys. Rev. C, 102, 034615 (2020).
8. Marini P., Taieb J., Laurent B. et al. Phys. Rev. C, 101, 044614 (2020).
9. Gerasimenko B., Drapchinsky L., Kostochkin O., et al. J. Nucl. Sci. Technol. 2, 362 (2002).
10. Kornilov N.V., Kagalenko A.B., Hambsch F.-J. Yad. Fiz. 62, 209 (1999).
11. Watt B.E. Phys. Rev., 87, 1037 (1952).
12. Maslov V.M. Yad. Fiz. 71, 11 (2008).
13. Maslov V.M. In: Proc. LXXIII Intern. Conf. "Nucleus 2023", Fundamental problems and applications, Sarov, 8—13 October 2023, Book of abstracts, p. 119, http://book.sarov.ru/wp-content/uploads/2023/11/ Nucleus-2023-73-conference-abstracts.pdf.
14. Devlin M., Bennett E.A., Buckner M.Q. et al. In: Proc. Intern. Conf. Nuclear Data for Science and Technology, July 24—29, 2022, Sacramento, USA; https://indico.frib.msu.edu/event/52/ contributions/616/ attachments/491/2023/ Devlin -ND2022.pdf; Eur. Phys. Journ. Web of Conf., 284, 04007 (2023).
15. Brown D., Chadwick M., Capote R. et al. Nuclear Data Sheets, 148, 1 (2018).
16. Shibata K., Iwamoto O., Nakagawa T. et al. J. Nucl. Sci. Technol., 48, 1 (2011).
17. Kornilov N.V. Vopr. At. Nauki Tech., Ser. Yad. Const. 4, 46 (1985).
18. Lovchikova G.N., Trufanov A.M., Svirin M.I. et al. Yad. Fyz. 67, 1270 (2004).
19. Trufanov A.M., Lovchikova G.N., Svirin M.I. et al. Yad. Fiz. 64, 3 (2001).